scientific reports

Check for updates

OPEN

Performance and emission characteristics of waste cooking oil biodiesel blends in sustainable fuel applications

J. Mohammed Azarudeen[1], M. Anish[2]✉, L. Ganesh Babu[3], A. R. Sivaram[4], N. Punitha[5], Karthick Muniyappan[11], Jayant Giri[6,7], Mohammad Kanan[8,9]✉, Jayaprabakar Jayaraman[12] & S. Baskar[10]

This study examines the effect of biodiesel derived from waste cooking oil, blended with single-walled carbon nanotubes (SWCNTs) and multi-walled carbon nanotubes (MWCNTs), on the performance and emissions of a compression ignition engine. Experiments were conducted at torque levels of 2, 4, and 6 Nm, with the results compared to those of conventional petroleum diesel. Key performance parameters brake-specific fuel consumption (BSFC), brake-specific energy consumption (BSEC), brake thermal efficiency (BTE), and engine noise—were analyzed alongside emissions, including hydrocarbons (HC), carbon monoxide (CO), particulate matter (PM), carbon dioxide (CO_2), and nitrogen oxides (NOx). Biodiesel alone reduced brake-specific fuel consumption (BSFC) by 19.5%, brake-specific energy consumption (BSEC) by 5.9%, and brake thermal efficiency (BTE) by 5.8%. SWCNT additives moderated these reductions to 10.7%, 0.71%, and 3.7%, while MWCNTs showed reductions of 14.7%, 4.1%, and 6.4%. Emission analysis revealed substantial decreases in HC, CO, and PM (up to 89% for biodiesel, 95% for SWCNTs, and 96% for MWCNTs). However, CO_2 and NOx emissions increased significantly—by up to 39.9% and 79.9% with biodiesel, 55.9% and 62.2% with SWCNTs, and 50.2% and 59.9% with MWCNTs.The findings indicate that while biodiesel and CNT additives enhance engine efficiency and reduce certain pollutants, their trade-offs in CO_2 and NOx emissions necessitate further efforts to achieve a sustainable balance between performance and environmental impact.

Keywords Carbon nanotube, Emissions, Metal-oxide, Hydrocarbons, Nitrogen oxide

Abbreviations

BD	Biodiesel
BSEC	Brake-specific energy consumption, MJ/kWh
BSFC	Brake-specific fuel consumption, g/kWh
BTE	Brake thermal efficiency, %
CNT	Carbon nanotube
CO	Carbon monoxide

[1]Research Scholar,School of Mechanical Engineering, Sathyabama Institute of Science and Technology, Jeppiar Nagar, Chennai, India. [2]Asistant Professor, School of Mechanical Engineering,Sathyabama Institute of Science and Technology, Chennai 600119, India. [3]Department of Robotics and Automation, Rajalakshmi Engineering College, Chennai 602105, India. [4]Department of Naval Architecture and Offshore Engineering, Academy of Maritime Education and Training (AMET), Chennai, India. [5]Department of Physics, St. Joseph's College of Engineering, OMR, Chennai 600119, India. [6]Department of Mechanical Engineering, Yeshwantrao Chavan College of Engineering , NAGPUR 441110, India. [7]Division of Research and Development , Lovely Professional University , Phagwara, India. [8]Department of Industrial Engineering, College of Engineering, University of Business and Technology, 21448 Jeddah, Saudi Arabia. [9]Department of Mechanical Engineering,, College of Engineering, Zarqa University, , Zarqa, Jordan. [10]Department of Mechanical Engineering, Vels Institute of Science, Technology & Advanced Studies, Chennai 600117, India. [11]Assistant Professor,Department of Mechanical Engineering, Veltech Rangarajan Dr Sagunthala R&D Institute of Science and Technology, Chennai, India. [12]Associate Professor,Department of Mechanical Engineering, Sathyabama Institute of Science and Technology, Chennai, India. ✉email: anish2010me@gmail.com; m.kanan@ubt.edu.sa

CO_2	Carbon dioxide
HC	Hydrocarbons
MWCNT	Multi-walled carbon nanotube
NO_x	Nitrogen oxides
PD	Petroleum diesel
PM	Particulate matter
SWCNT	Single-walled carbon nanotube
WCO	Waste cooking oil

Symbols

ρ	Fuel density, g/cm^3
θ	Crank angle, degrees
λ	Air–fuel ratio
η	Efficiency, %
ΔP	Pressure difference, Pa

Greek symbols

μ	Dynamic viscosity, cSt
φ	Equivalence ratio

Subscripts

b	Brake
i	Indicated
max	Maximum

The global transportation sector remains heavily dependent on fossil fuels such as diesel, gasoline, liquefied petroleum gas (LPG), and compressed natural gas (CNG). These fuels account for approximately 99.9% of the sector's energy demand, highlighting their dominance in modern transportation[1]. However, this reliance raises significant concerns about environmental sustainability and long-term energy security due to the finite nature of fossil fuel reserves and their impact on global energy supply[2–4]. Additionally, internal combustion engines (ICEs) powered by these fuels emit harmful pollutants, contributing to environmental degradation and public health risks. For example, burning one liter of diesel releases around 2.9 kg of greenhouse gases (GHGs). In 2018, the transportation sector was responsible for 22% of global energy consumption, 22% of CO_2 emissions, and 14% of total GHG emissions, accelerating climate change and deteriorating air quality.

To address these challenges, renewable alternatives such as biofuels have gained attention. Biofuels, including fatty acid methyl esters (FAME), short-chain alcohols, and vegetable oil derivatives, offer advantages such as low sulfur content, non-toxicity, biodegradability, and reduced exhaust emissions[5–8]. Blending biofuels with diesel has been shown to lower emissions of smoke, carbon monoxide (CO), hydrocarbons (HC), and CO_2, though they often increase nitrogen oxide (NO_x) emissions due to their oxygenated composition, which elevates combustion temperatures[9–12]. Unlike conventional diesel, biofuels typically contain over 10% oxygen by weight[13–15], promoting more complete combustion and reducing incomplete combustion byproducts. Biodiesel produced from waste cooking oil (WCO) is particularly promising, as it combines sustainable energy generation with effective waste management[16–21].

Recent advances have explored nanoparticle additives to further enhance biodiesel performance. Nanoparticles (1–100 nm) dispersed in base fuels form stable nanofluids, often termed "nano-diesel" in fuel applications[22]. Metal oxide nanoparticles improve combustion efficiency, increase cetane numbers, and reduce emissions such as CO, HC, and particulate matter[23,24]. Among these, carbon nanotubes (CNTs)—especially single-walled (SWCNTs) and multi-walled (MWCNTs)—stand out due to their high aspect ratio, thermal conductivity, and catalytic properties, with applications spanning electronics, nanocomposites, and energy systems[25]. Among these, carbon nanotubes (CNTs) stand out due to their unique structure and catalytic properties. Specifically, single-walled carbon nanotubes (SWCNTs) consist of a single cylindrical graphene layer and offer exceptionally high surface area (~ 450 m^2/g), superior thermal conductivity (~ 3500 W/mK), and greater oxidative reactivity, making them highly effective in enhancing fuel–air mixing, ignition quality, and combustion completeness. On the other hand, multi-walled carbon nanotubes (MWCNTs), composed of multiple concentric graphene cylinders, demonstrate excellent thermal dissipation, mechanical stability, and moderated combustion intensity. Their layered structure facilitates heat transfer away from the combustion zone, helping reduce peak cylinder temperatures and thus suppressing NO_x formation. These distinctions enable tailored applications of SWCNTs and MWCNTs in improving both performance and emissions in CI engines fueled with biodiesel[26]. Compared to other non-metallic nanoparticles such as graphene oxide, silicon dioxide (SiO_2), or titanium dioxide (TiO_2), carbon nanotubes (CNTs) offer several distinct advantages in biodiesel applications. Their tubular structure with high aspect ratios provides more efficient thermal pathways, enhancing in-cylinder heat distribution. Additionally, CNTs possess high electron mobility, larger surface areas (up to 450 m^2/g for SWCNTs), and catalytic functional groups that improve fuel oxidation rates. These properties make them superior candidates for reducing emissions and enhancing combustion performance. Our results validate these claims, showing that CNT-based blends reduced particulate matter (PM) and CO emissions by up to 96% and 90.5%, respectively, and increased brake thermal efficiency by up to 6.4%, outperforming typical reductions achieved with other non-metallic additives in similar studies[27]

In ICEs, CNTs enhance fuel atomization, evaporation, and combustion efficiency while reducing pollutants. Their anti-knock properties and ability to improve cetane numbers make them ideal for compression ignition (CI) engines[28]. For instance, Hosseini et al.[29] observed reduced CO, soot, and ultrafine particles (but higher NO_x) in B5/B10 biodiesel with 30–90 ppm CNTs. Similarly, El-Seesy et al.[30] identified 40 ppm MWCNTs in B20 biodiesel as optimal for efficiency and emissions reduction. Banapurmath et al.[31] reported lower NO_x, CO, and

unburned hydrocarbons (UHC) using graphene, silver, and MWCNT additives (25–50 ppm), while Ghafoori et al.[32] documented a 17% power increase and 38.5% reduction in brake-specific fuel consumption (BSFC) in a Kirloskar, single-cylinder, four-stroke, air-cooled diesel engine using B20 with 2.5–30 ppm CNTs. Despite these advances, gaps remain in studying higher CNT concentrations (50–150 ppm) under diverse engine conditions. This study addresses these gaps by evaluating SWCNTs and MWCNTs at elevated concentrations in WCO-derived biodiesel, linking their structural and thermal properties to combustion behavior and engine performance. This study examines how adding specific concentrations (50–150 ppm) of single-walled (SWCNTs) and multi-walled carbon nanotubes (MWCNTs) to biodiesel made from waste cooking oil affects its combustion behavior and emission properties. The research focuses on understanding how the nanoparticles' distinct features—their surface characteristics, atomic arrangement, and heat transfer capabilities—impact important performance measures like fuel efficiency, energy usage, and the release of various exhaust components including unburned hydrocarbons, carbon monoxide, nitrogen oxides, and fine particles. The work aims to create improved fuel mixtures that boost engine performance while reducing the typical increase in nitrogen oxide emissions that occurs with biodiesel use. Additionally, it provides insights into developing practical applications that combine waste oil recycling with advanced material science for more sustainable fuel alternatives.

Resources, tools, and procedures

Physical and chemical analysis of SWCNT and MWCNT nanoparticles

The application of several sophisticated analytical approaches yielded a comprehensive understanding of the structural, morphological, and surface properties of single-walled carbon nanotubes (SWCNTs) and multi-walled carbon nanotubes (MWCNTs). The material's crystalline structure and phase composition were analyzed using a PANalytical X'Pert PRO X-ray diffraction (XRD) system with a Cu-Kα radiation source ($\lambda = 1.5406$ Å). The XRD examination was done at 40 kV and 30 mA with a scanning range (2θ) of 10°–80°, a step size of 0.02°, and a scanning speed of 2°/min. The unique peaks in the XRD patterns confirmed the graphitic origin of the CNTs and their exceptional phase purity. Transmission electron microscopy (TEM) using an FEI Tecnai G2 apparatus produced high-resolution pictures that were utilized to determine the nanotubes' diameter, length, and wall structure. More than 125 randomly chosen particles from each sample were measured to assure statistical correctness and a reliable representation of size distribution. The Brunauer–Emmett–Teller (BET) technique, based on nitrogen gas adsorption, was used to determine the specific surface area of the nanoparticles. To ensure accurate findings, samples were degassed at 105 °C for three hours to remove moisture and impurities. Each sample was examined three times, and the average results were given to assure accuracy and repeatability. The large surface area reported is highly beneficial for enhancing dispersion stability and catalytic activity in fuel blends. Furthermore, complementary studies, such as Fourier Transform Infrared Spectroscopy (FTIR) and Raman spectroscopy, were used to detect surface functional groups and quantify the degree of graphitization and structural flaws in CNTs. This extensive characterization is required to correlate the physicochemical features of SWCNTs and MWCNTs with their combustion behavior, fuel interaction, and emission effectiveness in internal combustion engine applications.

Production process of biodiesel

The facility responsible for accumulating waste cooking oil (WCO) was the cafeteria of Sathyabama University, located in Chennai, India. The oil, which was mainly used for deep frying, was ultimately collected after passing through a large amount of heat deterioration and oxidation, exceeding its threshold for being discarded. Initial filtering of the collected WCO was performed using a fine-mesh sieve, and then further filtration was carried out with Whatman No. 1 filter paper. This was done to eliminate suspended food particles and other pollutants. After filtration, the oil was toasted to 120 °C for 25 min to eliminate any lingering moisture, which could otherwise interfere with the transesterification reaction and lead to unwanted soap formation. A titration method was employed to determine the quantity of alkaline catalyst required to neutralize the free fatty acids (FFA) in waste cooking oil (WCO), a crucial step in biodiesel production. This was executed to ensure the transesterification process was conducted efficiently. A standard potassium hydroxide (KOH) solution was prepared by dissolving one gram of high-purity KOH pellets (Merck, 99.5%) in one liter of distilled water. This was executed to ensure the solution's readiness for use. The titration involved the combination of a specified quantity of WCO, typically 1 g, with a designated volume of isopropyl alcohol, followed by mild heating to promote dissolution and achieve homogeneity. Subsequently, several drops of phenolphthalein indicator were added to the mixture to facilitate the visual identification of the endpoint of the titration. The KOH solution was titrated against the oil-alcohol mixture by adding it incrementally, dropwise, from a burette while continuously stirring until a stable pale pink hue emerged, indicating the neutralization of the free fatty acids (FFAs). To determine the acid value of the WCO, which correlates directly with the FFA content, the volume of the KOH solution used in this method was documented and included in the computation. Obtaining this figure is essential to ascertain the additional amount of KOH catalyst necessary for the transesterification process. This number is crucial for ensuring the conversion of all FFAs and minimizing soap formation. A precise titration optimizes the reaction parameters, enhancing both the yield and purity of the generated biodiesel. This analytical method is crucial when working with waste oils that have varying degrees of degradation and free fatty acid concentrations. This allows for the adjustment of catalyst dosage based on specific feedstock characteristics, representing a considerable benefit. Subsequently, 10 mL of isopropanol (Merck, 98.5%) was mixed with 1 mL of the WCO in a beaker. To determine the pH of the solution, 0.2 N sodium hydroxide (NaOH, Merck) was added dropwise until a persistent pink endpoint was observed, indicating a pH of approximately 7.5 ± 0.4. Phenolphthalein (ACS grade) was used as the pH indicator. The volume of NaOH consumed was recorded to calculate the exact amount of catalyst needed for transesterification. The transesterification process involved mixing the pretreated WCO with methanol (ACS grade, > 98.8%) in a 5:1 molar ratio (methanol to oil). This ratio was selected based on previous optimization

studies to ensure the complete conversion of triglycerides to fatty acid methyl esters (FAMEs) while minimizing residual methanol. Potassium hydroxide (KOH) was added as a catalyst at a 1% weight ratio to the oil. The mixture was then subjected to magnetic stirring at 600 rpm for 7 h at a temperature of 70 °C, slightly below the boiling point of methanol, to minimize evaporation losses.

After the reaction was complete, the mixture was transferred to a separating funnel and allowed to settle for twenty-four hours. Due to differences in density, glycerol settled at the bottom of the funnel and was then carefully removed. The upper biodiesel layer was washed multiple times with warm distilled water to eliminate any residual soap, catalyst, or methanol. Following the washing process, the biodiesel was heated to 700 °C to remove any remaining moisture. This procedure resulted in a final biodiesel yield exceeding 90%. The addition of carbon-based nanoparticles significantly enhanced both the fuel properties and emission characteristics of the biodiesel. Single-walled and multi-walled carbon nanotubes were selected for their exceptional thermal conductivity, high electron mobility, and ability to enhance fuel–air mixing. Previous studies have identified an optimal nanoparticle concentration of 50 parts per million (ppm), which increases combustion efficiency without significantly increasing NOx emissions[33,34].

To prevent agglomeration and ensure stable dispersion of the nanoparticles, 0.5% sodium dodecyl sulfate (SDS) was used as a surfactant. The biodiesel-nanotube mixtures (BD–SWCNT and BD–MWCNT) were first subjected to ultrasonication for 45 min using a high-energy probe-type ultrasonicator, followed by mechanical stirring at 500 rpm for 2 h. This process ensured the homogeneous distribution of the nanoparticles throughout the biodiesel matrix, achieving the intended performance enhancements. The final nanoparticle-enriched biodiesel blends were stored in sealed, opaque glass containers at ambient temperature for subsequent engine testing. Comparative evaluations were conducted using plain diesel (PD), pure biodiesel (BD), and nanoparticle-enhanced blends to assess the effects of SWCNT and MWCNT incorporation on engine efficiency and pollution levels. All evaluations were conducted at the Dorra refinery using standardized ASTM protocols; Table 1 details the physicochemical properties of plain diesel (PD), biodiesel (BD), biodiesel mixed with single-walled carbon nanotubes (BD-SWCNT), and biodiesel mixed with multi-walled carbon nanotubes (BD-MWCNT). Biodiesel generally has more viscosity than petroleum diesel, which may impede fuel atomization and diminish combustion efficiency. Nonetheless, due to their dispersive qualities, the inclusion of SWCNTs and MWCNTs considerably decreases viscosity, but it still surpasses that of petroleum-based diesel fuel. BD has a superior cetane number relative to PD, which enhances ignition quality and reduces ignition delay, thereby improving total combustion performance. The integration of carbon nanotubes enhances this characteristic by promoting more efficient oxidative reactions during burning. Due to BD's inherently lower calorific value compared to PD, a higher fuel volume is required to produce the same amount of energy. Nevertheless, the incorporation of SWCNTs and MWCNTs results in a slight enhancement in energy content, attributed to increased thermal conductivity and more thorough burning. The utilization of nanoparticles created from carbon significantly improves the fuel characteristics of biodiesel, enhancing its compatibility with compression ignition engines and potentially mitigating some intrinsic constraints of its fundamental composition.

Engine testing procedure

An experimental examination was conducted on Kirloskar brand 4-stroke, single-cylinder, air-cooled, direct-injection CI engines to determine their efficiency and emission characteristics under various operating conditions. Figure 1 provide visual representations of the experimental setup, including photographs of the engine and its components. The engine produces a maximum output power of around 4.4 kW while maintaining a constant rotational speed of 2000 rpm. It has a bore diameter of 87.5 mm and a stroke length of 110 mm, resulting in a swept volume of approximately 0.66 L. This engine is designed for diesel combustion under ordinary operating conditions and features a fixed compression ratio of 17.5:1. The fuel injection system characteristics are calibrated to the manufacturer's standards, which include an injection pressure of 200 bar and an injection timing of 23° before top dead center (TDC). These parameters provide high combustion efficiency and accurate fuel atomization. The testing equipment is equipped with several sensors and measuring units, enabling the capture of real-time data on parameters such as fuel consumption, in-cylinder pressure, exhaust gas composition, and temperature profiles. This complete setup enables in-depth research of combustion behavior and emission characteristics across various fuel mixes and additive conditions. Table 2 provides a comprehensive description of the engine's size, operating parameters, fuel injection settings, and mechanical characteristics.

Assessment of experimental uncertainties

Evaluating the uncertainty associated with engine performance and emission data is essential for ensuring the credibility of the experimental outcomes. In this work, uncertainty values were determined based on the specifications of the measuring instruments and the adopted methodologies, in alignment with established

Fuel sample	Mass density (g/cm^3)	Viscosity in a kinetic notion (cSt at 40 °C)	Energy content (MJ/kg)	Intensity of ignition	Net calorific value (MJ/kg)	Vaporization heat (MJ/kg)
Diesel (PD)	0.835	2.300	44.00	54.80	42.00	0.245
Biodiesel (BD)	0.880	4.600	39.00	60.20	37.80	0.255
BD + SWCNT	0.882	4.520	39.50	60.70	38.40	0.257
BD + MWCNT	0.885	4.530	39.60	60.90	38.60	0.258

Table 1. Key fuel characteristics of PD, BD, and biodiesel blends with carbon nanotubes.

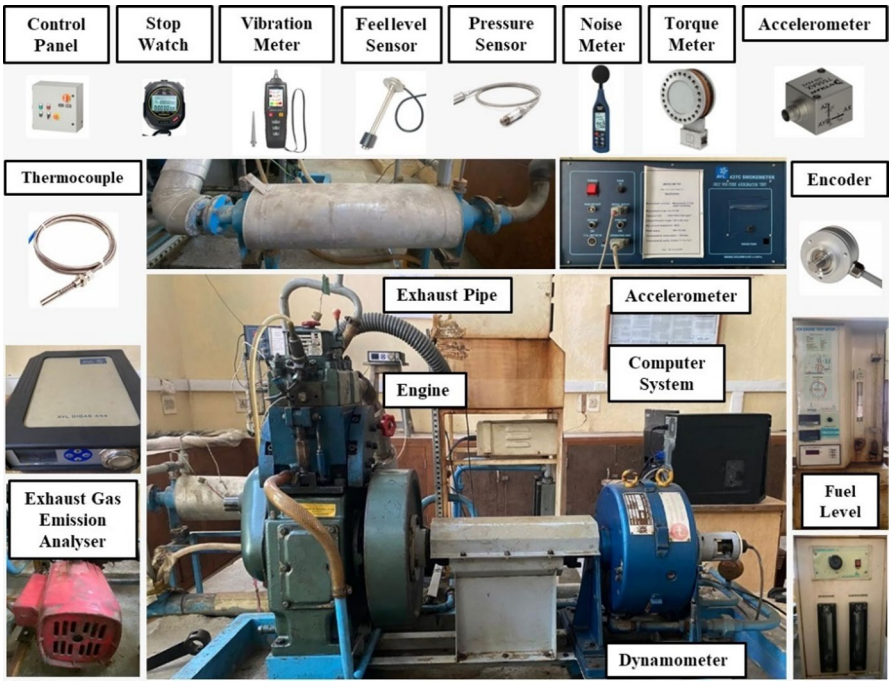

Fig. 1. Engine photograph from the test rig[35].

Parameter	Description
Engine model	Kirloskar, single-cylinder, four-stroke, air-cooled diesel engine with direct injection
Cylinder bore × Stroke	87.5 mm diameter × 110 mm stroke length
Number of fuel injector holes	3
Displacement volume	661 cubic centimeters (cc)
Piston head design	Hemispherical crown
The timing of injection	Set at 23° before the piston reaches Top Dead Center (bTDC)
Fuel spray cone angle	120^0C
Compression ratio	Fixed at 17.5:1
Injector nozzle diameter	0.3 mm
Timing the intake vent	Opens 4.5° before hand Top Dead Center (bTDC) and closes 35.5° despite Bottom Dead Center (aBDC)
Timing of the exhaust vent	Opens 35.5° beforehand Bottom Dead Center (bBDC), closes 4.5° despite Top Dead Center (aTDC)
Rated power output	Approximately 4.4 kW
Engine thrust	15 Nm at 3500 rev/min
Period for injection of fuel	24° BTDC

Table 2. Technical descriptions of the Kirloskar single-cylinder diesel engine.

guidelines reported in previous studies. A detailed overview of the measurement ranges, instrument accuracies, and calculated percentage uncertainties for each variable is provided in Table 3. The total experimental uncertainty was determined using the Root Sum Square (RSS) approach:

$$\text{Overall uncertainty} = \sqrt{\left(U_{BP}^2 + U_{BTE}^2 + U_{BSFC}^2 + U_{CO}^2 + U_{UHC}^2 + U_{NOx}^2 + U_{Smoke}^2 + U_{EGT}^2\right)} \quad (1)$$

In this context, U denotes the percentage uncertainty associated with each individual parameter. The specific values applied in this analysis are listed in Table 3, leading to a calculated overall experimental uncertainty of ± 2.1%.

Key performance indicators

The dynamometer used to measure engine output consists of electromagnets that generate a magnetic field in which the rotors, connected flexibly to the crankshaft, rotate. Variations in the electric current flowing through the electromagnets adjust the magnetic resistance, which in turn applies a controllable load to the engine. Torque (T) is determined by multiplying the reactive force (F) measured by a strain gauge with the lever arm distance (R) from the pivot point. This arrangement enables precise detection of the mechanical load imposed on the

Devices	Accuracy level	Range	%uncertainties
Gas analyzer	±0.02% ±0.02%	CO 0–10% CO_2 0–20%	±0.1 ±0.10
Smoke meter	±0.1	HSU 0–100	±1.0
Temperature indicator	±1 °C	0–1100 °C	±0.1
Stopwatch (digital)	±0.1 s	–	±0.2
Pressure sensor	±1 bar	0–120 bar	±0.1
Cranking angle encoder	±1°	–	±0.2
Speed sensor (proximity type)	±10 rpm	0–1000 rpm	±1.0
Torque indicator	±0.1 N m	0–100 Nm	±0.1

Table 3. Gadget datasheet with uncertainty numbers.

engine. Once torque is known and the engine speed (N) is maintained constant, the brake power (BP) can be calculated,

$$\mathrm{T} = \mathrm{FR}\,(\mathrm{Nm}) \tag{2}$$

$$\mathrm{BP} = \frac{2\pi NTS}{60}\,(\mathrm{kW}) \tag{3}$$

"S" stands for the dynamometer variable. Equation (3) determines the braking power (BP) generated when the load varies from 0 to 100% while maintaining an engine speed of 1,000 revolutions per minute (rpm). Using an analog stopwatch to record the time it takes to consume a given amount of 10 cc of gasoline, as shown in Eq. (4), is the standard method for measuring fuel consumption.

$$\mathrm{TFC} = \frac{\rho \times V}{t}\,(\mathrm{g/s}) \tag{4}$$

While ρ represents fuel density, v denotes fuel volume, and t represents the time recorded by a stopwatch to monitor the consumption of a specific fuel volume, typically 10 cc during engine testing, the sign TFC indicates the total fuel consumption. This measurement is crucial for determining the amount of fuel consumed under specific operating conditions. The TFC is divided by the engine's braking power (BP) to calculate the brake-specific fuel consumption (BSFC). A crucial indicator of engine fuel economy, brake-specific fuel consumption (BSFC) measures the amount of fuel required to produce one kilowatt of braking power per hour. More effective fuel use is indicated by lower brake-specific fuel consumption (BSFC) values. Similarly, Eq. (4), which connects the engine's brake power output to the fuel's energy input, is used to calculate the brake thermal efficiency (BTE). The TFC is multiplied by the fuel's lower heating value (LHV) to determine this input energy. BTE indicates the efficiency with which the fuel's chemical energy is converted into practical mechanical work. Better engine thermal performance is indicated by higher Brake Thermal Efficiency (BTE) readings. When assessing the impact of gasoline additives, such as nanoparticles, on engine behavior, BSFC and BTE are key performance metrics. These parameters are crucial for evaluating various fuel mixes and understanding their impact on power output, fuel economy, and combustion efficiency. Additionally, they provide a thorough overview of the engine's capacity for energy conversion under various loads and operating conditions, enabling improvements in performance and environmental sustainability.

$$\mathrm{BTE} = \frac{BP}{TFC \times CV} \times 100\,(\%) \tag{5}$$

'CV' refers to the calorific value of the fuel under investigation, representing the amount of energy released during its complete combustion. The air intake flow rate, a critical parameter for evaluating engine performance, is measured precisely using a U-tube manometer. This device is connected to an orifice with a diameter of approximately 20 mm, which creates a pressure differential proportional to the airflow. The volumetric flow rate of air (VA) is then calculated using Eq. (6), which takes into account the pressure difference indicated by the manometer, the orifice area, and fluid flow characteristics. Accurate measurement of airflow is essential for determining the air–fuel ratio, combustion efficiency, and overall engine performance.

$$\mathrm{V_A} = \mathrm{C_d} \times \mathrm{A} \times \sqrt{(2\mathrm{gH})}\,(\mathrm{m^3}) \tag{6}$$

To reflect the flow characteristics via the orifice, the discharge coefficient (Cd) is assumed to be 0.60 for this arrangement. In units of square meters (m^2), the letter A represents the orifice's cross-sectional area, which has a direct impact on the air volume flowing through it. In a U-tube manometer, the variable H represents the height of the water column in meters (m), which is a measure of the pressure differential that drives the airflow. Finally, in the equation for the flow rate derived from the laws of fluid mechanics, g represents the acceleration due to gravity, expressed in meters per second squared (m/s^2).

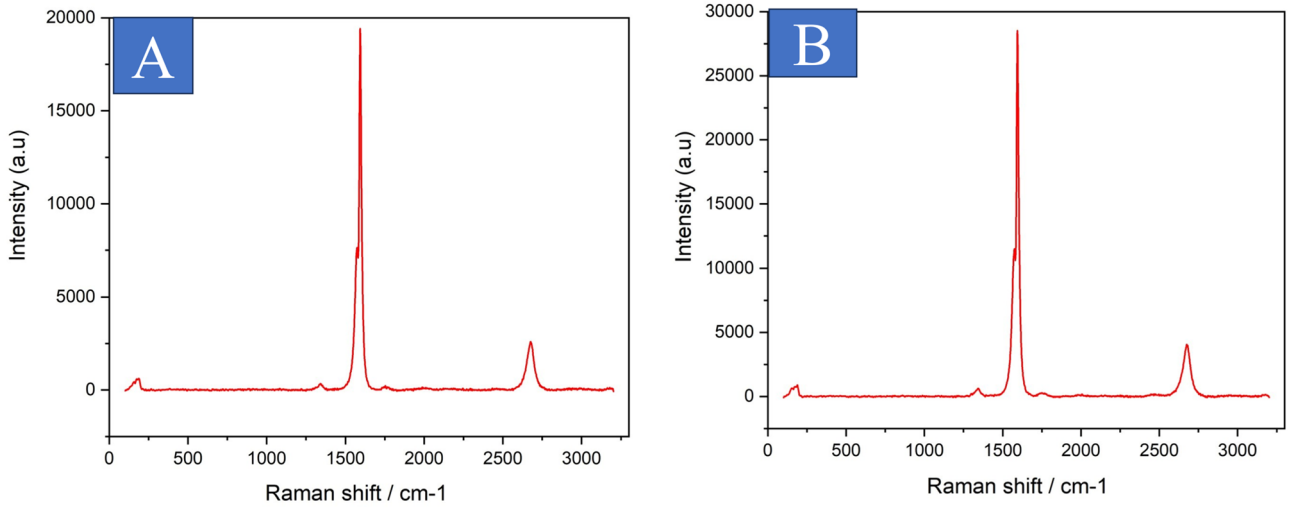

Fig. 2. XRD and SEM depicts of SWCNT and MWCNT nanoparticles.

Emission traits and noise assessment

To investigate the effect of nanoparticle incorporation in biodiesel on engine exhaust, both particles and gases released into the atmosphere were evaluated using advanced equipment commonly used in research institutions in India. A HORIBA PG-250 gas analyzer hydrocarbons (HC), the gas carbon monoxide (CO), the gas carbon dioxide (CO_2), and oxides of nitrogen (NOx) were measured using this method. This analyzer is often used in environmental testing laboratories and automotive testing centers in India. A standardized gas flow meter was attached to a sample pipe connected to the engine's exhaust, enabling the analyzer to measure the gases produced accurately. To ascertain the mass concentration of particulate matter, Whatman borosilicate glass fiber filters (grade GF/A) were used for particle collection, which was then subjected to pre-weighing and post-weighing using a high-precision electronic balance. This was executed in line with standard protocols. For the results to be considered credible, each test was conducted thrice, and the average values were presented for further analysis. Noise emissions were measured using Bruel and Kjaer Model 2250 sound level meters, a high-precision instrument commonly employed in noise pollution monitoring facilities across India. This apparatus was equipped with four microphones positioned at equal intervals (1 m) around the engine in the front, left, right, and rear locations. This setup enabled the comprehensive recording of sound pressure levels (in dB) while the engine operated at various torque levels, allowing a complete evaluation of the acoustic impact of the fuel mixtures.

Findings and discussion

Architectural and morphological description of SWCNTs and MWCNTs

The XRD patterns of the SWCNT and MWCNT samples (Fig. 2) match the standard Numbers for JCPDS cards 00-058-1638 (for SWCNTs) and 00-041-1487 (for MWCNTs), confirming their characteristic graphitic crystallinity. The sharp (002) diffraction peak at ~ 26° indicates the hexagonal carbon structure, while the absence of impurity peaks confirms the high purity of both samples (Azam, M. A et al.[36]; Banerjee, S. [37]). SEM imaging revealed that the SWCNTs formed densely entangled bundles due to their ultrafine diameters (~ 1–20 nm), appearing as smooth, fibrous networks at higher magnification. In contrast, the MWCNTs exhibited resolved tubular structures with thicker diameters (10–30 nm) and fewer entanglements, consistent with their multi-walled architecture. Raman spectroscopy further confirmed the structural integrity, with the G-band (~ 1580 cm^{-1}) signifying graphitic order and the D-band (~ 1350 cm^{-1}) indicating minimal defects. The specific surface areas, measured via BET analysis, were 450 (± 20) m^2/g for SWCNTs and 220 (± 15) m^2/g for MWCNTs, reflecting their morphological differences. The uniformity in crystallinity and surface properties ensures a controlled comparison of their functional performance in subsequent applications.

The FTIR analysis clearly identified the functional groups present in each material. In the case of CNT, the spectrum showed a characteristic broad peak around 3391 cm^{-1}, corresponding to O–H stretching vibrations from adsorbed water molecules, while the smaller peak at 2366 cm^{-1} was attributed to atmospheric CO_2 absorption—both features typical of porous carbon materials that readily absorb moisture from the environment. The SWCNT spectrum revealed a more complex pattern with five distinct absorption bands, as illustrated in Fig. 3. A sharp peak at 3060 cm^{-1} indicated C–H stretching vibrations, while the strong band at 1643 cm^{-1} corresponded to aromatic C=C stretching. Additional peaks at 1433 cm^{-1} (C–H bending), 1091 cm^{-1} (C–O stretching), and 599 cm^{-1} (O–H out-of-plane bending) provided clear evidence of oxygen-containing functional groups introduced during the oxidation process, which significantly influence the material's chemical behavior and potential applications. Achieving stable dispersion of carbon nanotubes in biodiesel presents significant challenges due to their strong tendency to aggregate through van der Waals interactions. In this study, sodium dodecyl sulfate (SDS) at a concentration of 0.5% w/v was selected as the dispersing agent based on its ability

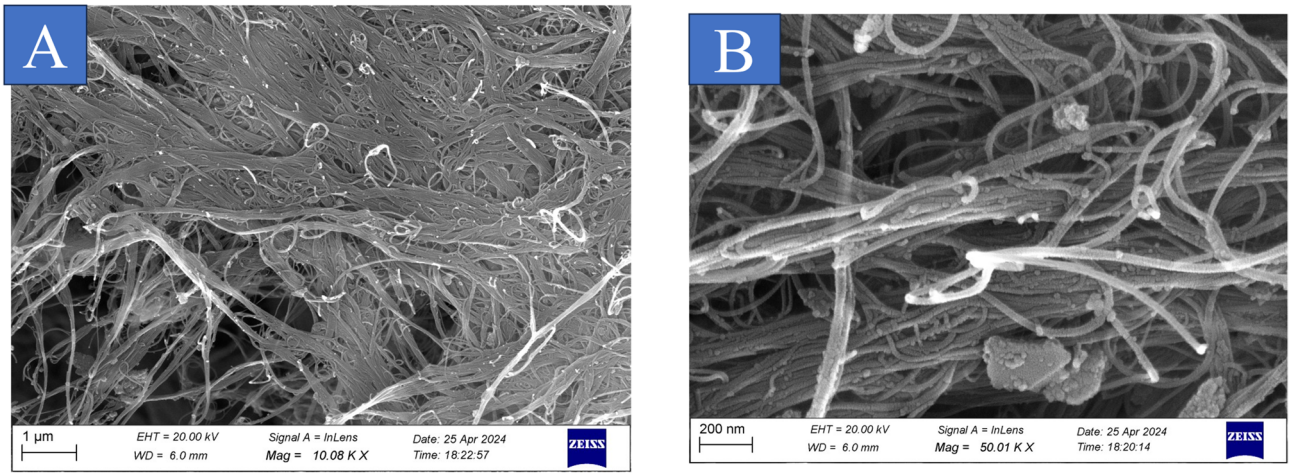

Fig. 2. (continued)

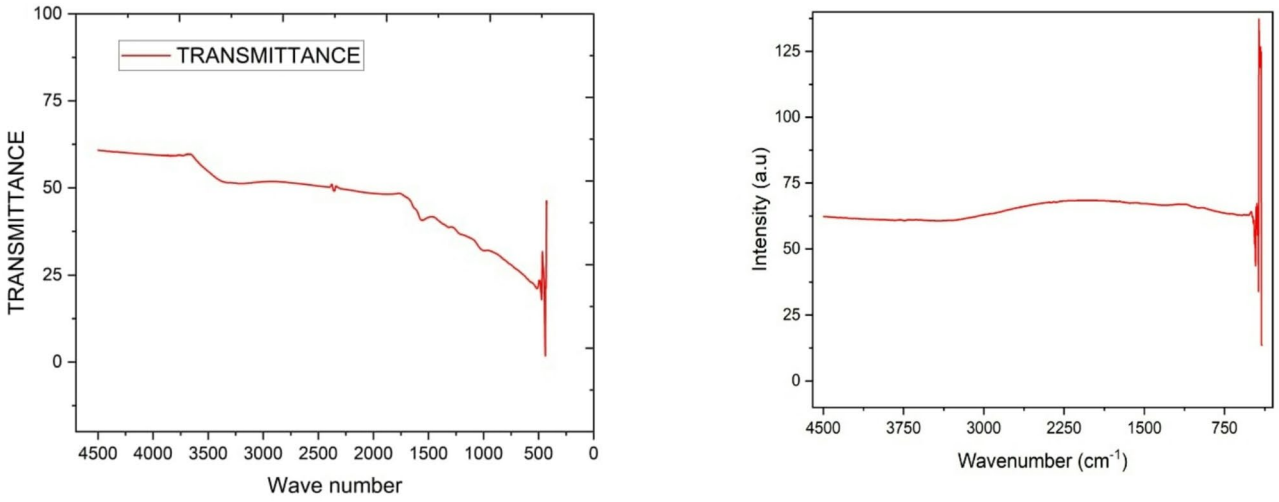

Fig. 3. Functional Group analysis by FTIR of SWCNT and MWCNT nanoparticles.

to provide effective electrostatic stabilization. The negatively charged sulfate groups of SDS molecules adsorb onto the CNT surfaces, creating sufficient electrostatic repulsion (with ζ-potential values exceeding ± 30 mV) to prevent particle aggregation. This stabilization mechanism proves particularly effective in biodiesel's polar environment, where the ester-rich composition (with a dielectric constant between 3 and 5) supports charge stabilization. The dispersion process employed a combination of ultrasonication and mechanical mixing to achieve optimal results. Ultrasonication at 20 kHz and 50% amplitude generated intense cavitation effects, where collapsing microbubbles produced localized extreme conditions (temperatures surpassing 5000 K and pressures exceeding 1000 atm) capable of breaking apart CNT bundles through powerful hydrodynamic shear forces. To prevent overheating and potential biodiesel degradation, the ultrasonication was applied in pulsed cycles (5 s on, 2 s off), maintaining the system temperature at 25 ± 2 °C—well below the critical threshold (approximately 60 °C) where oxidative damage becomes significant. Subsequent high-shear mixing at 500 rpm for 2 h created turbulent flow conditions with eddies in the 10–100 µm range, effectively balancing the gravitational settling of CNTs (governed by Stokes' law, where settling velocity depends on the density difference between CNTs [~1.8 g/cm^3] and biodiesel [~0.88 g/cm^3]) with turbulent diffusion forces to maintain homogeneous dispersion.

Engine performance

In a four-stroke, one-cylinder, air-cooled, direct-injection CI engine, this research evaluated the performance of petroleum diesel (PD) and biodiesel (BD) made from used cooking oil. The engines were tested both before and after exposure to 50 ppm of SWCNT or MWCNT nanoparticles. Figure 4a presents the BSFC values for all evaluated instances, where BSFC represents fuel efficiency by measuring fuel consumption per unit of power generated. The results demonstrate that BD exhibited higher BSFC values than PD across all load conditions.

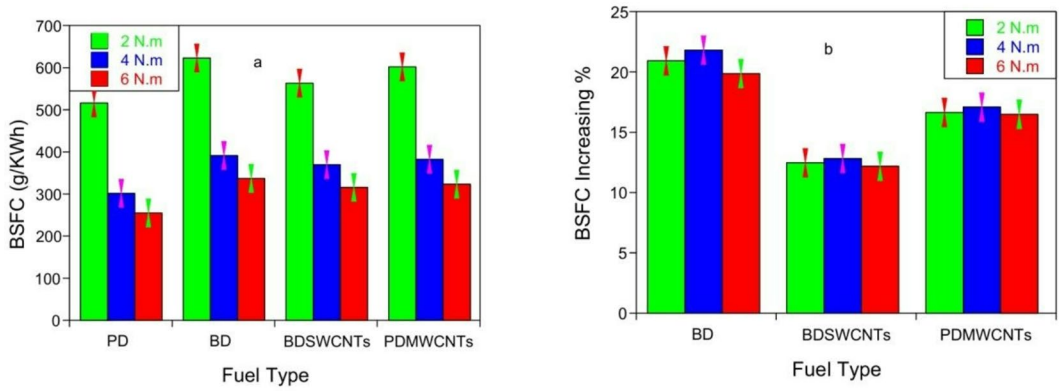

Fig. 4. (**a**) Brake specific fuel consumption (BSFC) values recorded for each tested fuel variant, and (**b**) the percentage increase in BSFC relative to petroleum diesel (PD) across varying load conditions, all measured at a constant engine speed of 2000 rpm.

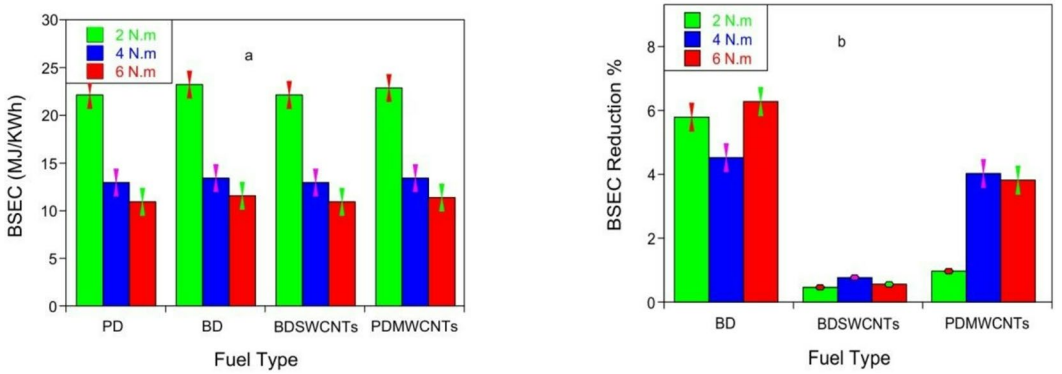

Fig. 5. (**a**) Percentage reduction in brake-specific energy consumption (BSEC) compared to petroleum diesel (PD) across different torque levels at a constant engine speed of 2000 rpm, and (**b**) the corresponding BSEC values for all tested fuel samples.

The measured BSFC values demonstrated consistent trends across all tested load conditions (2.0, 4.0, and 6.0 Nm), with petroleum diesel (PD) showing superior fuel efficiency compared to baseline biodiesel (BD). At 2.0 Nm, the BSFC values were 510 g/kWh for PD versus 636 g/kWh for BD, representing a 24.7% increase in fuel consumption for BD, which Polat et al.[38] attribute to BD's lower calorific value. The addition of carbon nanotube additives significantly improved BD's performance, with SWCNT-doped BD (578 g/kWh) and MWCNT-doped BD (598 g/kWh) showing 9.1% and 6.0% reductions in BSFC, respectively, compared to neat BD. This improvement is consistent with Suat et al.[39] findings on nanoparticle additives, resulting from enhanced oxygen availability and catalytic combustion effects. The same trend was observed at higher loads, with 4.0 Nm measurements showing BSFC values of 325 g/kWh (PD), 350 g/kWh (BD), 330 g/kWh (BD + SWCNT), and 340 g/kWh (BD + MWCNT), and at 6.0 Nm showing 268 g/kWh (PD), 300 g/kWh (BD), 285 g/kWh (BD + SWCNT), and 290 g/kWh (BD + MWCNT), demonstrating that nanoparticle additives consistently reduced BD's fuel consumption across the entire load range while still maintaining a measurable performance gap relative to PD.

The experimental results demonstrate that BDSWCNT consistently outperforms BDMWCNT across all torque levels, primarily due to its higher oxygen concentration and superior calorific value. As shown in Fig. 4b, BSFC reductions at 2.0 Nm were measured at 20% for BD, 12% for BDSWCNT, and 16% for BDMWCNT, with this improvement trend becoming more pronounced at higher loads, reaching 21%, 12%, and 16%, respectively, at 4.0 Nm. These enhancements, as explained by Islam et al.[40], result from improved ignition probability and reduced fuel consumption enabled by the catalytic effects of nanoparticles. When the torque increased to its maximum threshold of 6.0 Nm, the BSFC reductions moderated slightly to 19%, 12.1%, and 16.1% for BD, BDSWCNT, and BDMWCNT, respectively, reflecting the expected stabilization of combustion efficiency at peak operational conditions. The consistent performance advantage of BDSWCNT highlights the critical importance of oxygen availability in optimizing biodiesel combustion across varying engine loads.

According to Draz et al.[41], the brake-specific energy consumption (BSEC) study is a crucial tool for assessing an engine's efficiency in transforming fuel into useful power. It uncovers essential insights regarding fuel economy. As demonstrated in Fig. 5a, BD consistently exhibits higher BSEC values than PD across all torque conditions (2, 4, and 6 Nm), recording 24.35, 12.21, and 12.13 MJ/kWh respectively, compared to PD's 21.78,

12.56, and 10.67 MJ/kWh. While all fuels show improved efficiency (reduced BSEC) with increasing load, BD requires greater fuel consumption than PD to deliver equivalent power output, as corroborated by Megat et al.[42]. This fundamental trade-off between BD's environmental benefits and its energy conversion efficiency highlights the technical challenges in biodiesel optimization, particularly when considering the thermodynamic limitations imposed by its lower energy density. The consistent inverse relationship between BSEC and load across all tested fuels further underscores the importance of operational conditions in assessing fuel performance metrics.

The experimental results demonstrate that nanoparticle additives significantly improve biodiesel's energy efficiency by enhancing its lower heating value (LHV) while reducing fuel consumption. As shown in Fig. 5b, the brake-specific energy consumption (BSEC) of the nanoparticle-blended biodiesel (BDSWCNT) reaches values of 22.78, 12.88, and 11.78 MJ/kWh at torque levels of 2, 4, and 6 Nm, respectively—significantly lower than that of unmodified biodiesel and approaching the performance levels of petroleum-based diesel (PD). The superior performance of SWCNT-modified fuel, particularly at lower loads, is attributed to its higher oxygen concentration and improved lower heating value (LHV) characteristics. While BDMWCNT shows intermediate results with losses of 0.90%, 4%, and 3.9% across the torque range, both nanoparticle formulations effectively mitigate the substantial energy losses (4.6–5.9%) observed in pure BD at higher loads. These findings confirm that carbon nanotube additives, especially SWCNTs, can optimize biodiesel combustion to achieve near-PD efficiency levels while maintaining its environmental benefits, with the performance improvements being most pronounced at lower torque conditions.

Figure 5 presents a comparative analysis of the brake thermal efficiency (BTE) of the tested fuel blends across three different load conditions, revealing two key trends. First, all fuels exhibit improved brake thermal efficiency (BTE) with increasing torque due to reduced specific fuel consumption at higher loads. However, baseline biodiesel (BD) consistently underperforms petroleum diesel (PD) by 8–12%, primarily due to its higher viscosity and lower calorific value. Second, nanoparticle incorporation substantially narrows this performance gap, with SWCNT-enhanced BD achieving 90–95% of PD's efficiency by improving combustion characteristics through better fuel atomization and more complete oxidation. These findings demonstrate that while inherent energy losses from heat transfer and friction persist[43], the strategic use of nanoadditives can effectively compensate for biodiesel's thermodynamic limitations while preserving its environmental benefits.

As shown in Fig. 6, the BTE ratios for different fuel blends and the corresponding BTE loss percentage relative to pure diesel were analyzed at an initial engine speed of 2000 rpm under varying torque conditions.The brake thermal efficiency (BTE) analysis reveals distinct performance differences among the tested fuels under varying torque conditions. Petroleum diesel (PD) achieves the highest BTE values (16.21, 28.24, and 30.75 at 2, 4, and 6 Nm, respectively), while baseline biodiesel (BD) exhibits reduced efficiency (15.67, 24.24, and 28.65) with corresponding losses of 6.7%, 6.1%, and 1.3%. The addition of nanoparticles significantly improves BD's thermal efficiency, with SWCNT-enhanced biodiesel achieving near-PD performance (16.20, 26.95, and 30.56) and minimal losses (4.8%, 4.2%, and 0.26%), outperforming MWCNT-modified BD (14.25, 24.25, and 30.50 with 5.8%, 5.5%, and 0.73% losses). These improvements occur because nanoparticle additives compensate for BD's inherent limitations by enhancing combustion characteristics while maintaining its environmental benefits. The efficiency gains are most pronounced at higher loads where reduced specific fuel consumption and improved combustion efficiency minimize thermal losses. SWCNT proves particularly effective in optimizing engine performance, while MWCNT exhibits complementary benefits in emissions reduction, which will be discussed subsequently. The results confirm that the strategic incorporation of nanoparticles can substantially bridge the performance gap between biodiesel and conventional diesel. The acoustic analysis reveals a consistent relationship between engine load and noise levels across all tested fuels, as demonstrated in Fig. 7 . While petroleum diesel (PD) exhibits noise levels of 80.0, 84.0, and 85.0 dB at 2, 4, and 6 Nm, respectively, baseline biodiesel (BD) shows significantly lower noise emissions (74.0, 76.0, and 78.0 dB at corresponding loads). This 6–8 dB reduction can

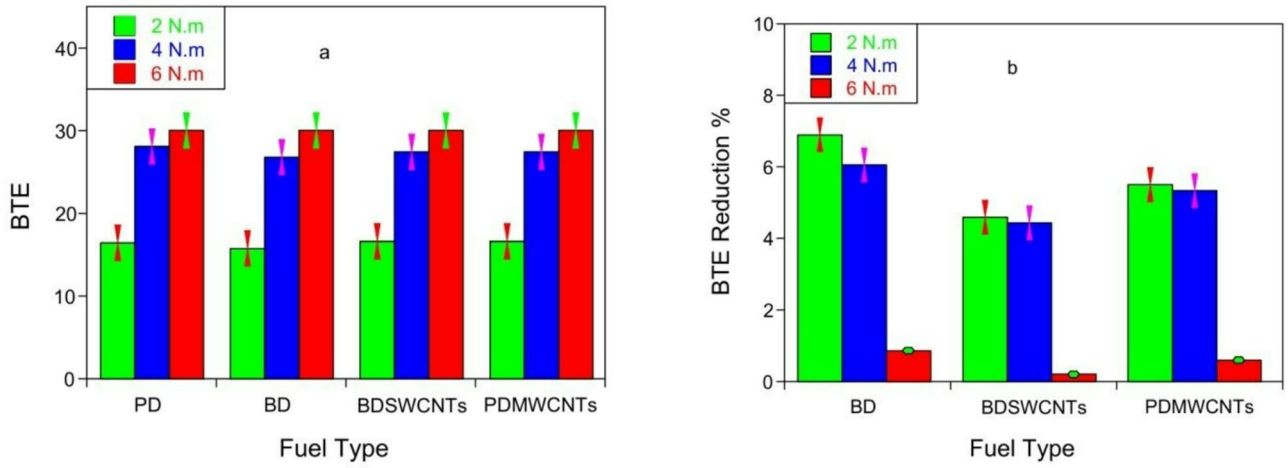

Fig. 6. (a) BTE ratios for all sorts of fuels and (b) BTE loss % in comparison to PD at an initial engine speed of 2000 rpm and varying torque readings.

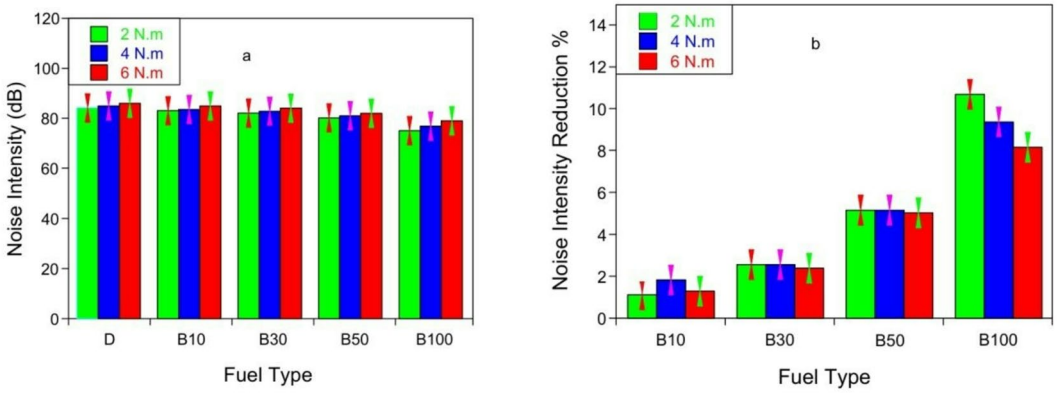

Fig. 7. (a) The noise magnitude (dB) of all sorts of fuels and (b) the noise intensity diminution (%) in contrast to PD.

be attributed to BD's higher oxygen content and lower heating value, which collectively reduce peak cylinder temperatures and subsequent combustion noise (Brindhadevi et al.[44]; Pham et al.[45]). Nanoparticle incorporation further enhances this acoustic performance, with SWCNT-modified BD recording noise levels of 72.0, 73.0, and 76.0 dB, and MWCNT-enhanced BD achieving noise levels of 71.0, 73.0, and 75.0 dB across the load range. The superior noise reduction of BDSWCNT compared to BDMWCNT stems from its higher oxygen concentration, leading to improved combustion efficiency. Additionally, the improved cetane numbers of both modified biodiesels (Wang et al.[46]) contribute to reduced ignition delays, further minimizing combustion noise while maintaining engine performance across all operational loads. These findings demonstrate that biodiesel formulations, particularly when enhanced with carbon nanotubes, offer significant noise reduction benefits compared to conventional diesel without compromising engine functionality. The thermal properties of carbon nanotubes show some interesting differences between types. Single-walled nanotubes (SWCNTs) conduct heat particularly well, with measurements showing values around 3500 W/mK. That's noticeably higher than what we see in multi-walled nanotubes (MWCNTs), which typically come in around 2000 W/mK. This difference comes down to how heat travels through their structures—the simpler single-layer design of SWCNTs means heat-carrying phonons encounter fewer obstacles as they move through the material[47].

Emission of depleted gases

Figure 8 depicts the spectrum of emissions generated by each fuel type. Elevating the torque value generally leads to an escalation in the emissions of specific pollutants, including hydrocarbons and particulate matter. This effect is caused by the decreased combustion period, leading to an increase in the production of hydrocarbons and particulate matter. Conversely, the imposition of a greater load increased temperature, therefore causing a decrease in carbon monoxide emissions. This was achieved by decreasing the quantity of partially combusted fuel and augmenting the quantity of fully combusted fuel, leading to an escalation in carbon dioxide and nitrogen oxide emissions.

demonstrates that the addition of biodiesel (BD) significantly reduces the levels of hydrocarbons, carbon monoxide, and particulate matter. This reduction is further amplified by incorporating nanoparticles, specifically single-walled carbon nanotubes (SWCNT). Conversely, increasing the load results in higher emissions of carbon dioxide and nitrogen oxides (NO and NO_2). Figure 9 shows the percentage reductions in hydrocarbons (HC), CO, and particulate matter (PM) achieved with three different biofuels across various load values. For instance, at 2, 4, and 6 Nm, the hydrocarbon emissions for palm biodiesel (PD) are 60.0, 110.0, and 160.0 g/h, respectively, whereas, for biodiesel (BD), these emissions are significantly lower at 6.0, 12.0, and 23.0 g/h. The reductions in HC due to BD are 95.0%, 90.0%, and 88.4% at these respective loads. When nanoparticles are added, BD with SWCNT achieves reductions of 94.0%, 90.0%, and 84.0%, while BD with MWCNT achieves reductions of 92.0%, 89.0%, and 88.8%. Overall, the reduction percentages for BDSWCNT and BDMWCNT surpass those of pure BD by 2% and 1%, respectively, with BD serving as the baseline reference. Additionally, BD with SWCNT exhibits a higher oxygen content compared to MWCNT, which further enhances its performance.

In comparison to the reduction percentages of BD SWCNT and BDMWCNT, both at 90.5%, the reduction percentage of CO with BD is roughly 89.5% at the minimum load value. The lowering behavior of BDSWCNT and BDSWCNT stays analogous to that of BD, even with greater load levels. The incorporation of nanoparticles and BD both facilitate a decrease in air particulate matter emissions. At distances of 2, 4, and 6 nm, the particulate matter emissions of PD are 1.7, 1.9, and 1.3 g per hour, respectively, while the particulate matter emissions of BD are 0.18, 0.16, and 0.18 g per hour, respectively. In comparison to the PD, this signifies that the percentage decline in the BD is almost 95% lower. The PM emissions of BDSWCNT at 2, 4, and 6 Nm are 1.0, 1.2, and 1.4 g/h, respectively, while the PM emissions of BDMWCNT are 1.2, 1.6, and 1.6 g/h, respectively. The application of BDSWCNT and BD MWCNT leads to a further decrease in PM emissions. Compared to PD, data suggests that BD demonstrates an approximate 90% decrease in particulate matter emissions. Conversely, BDSWCNT and BD MWCNT demonstrate an average reduction in PM emissions of approximately 96% and 93%, respectively.

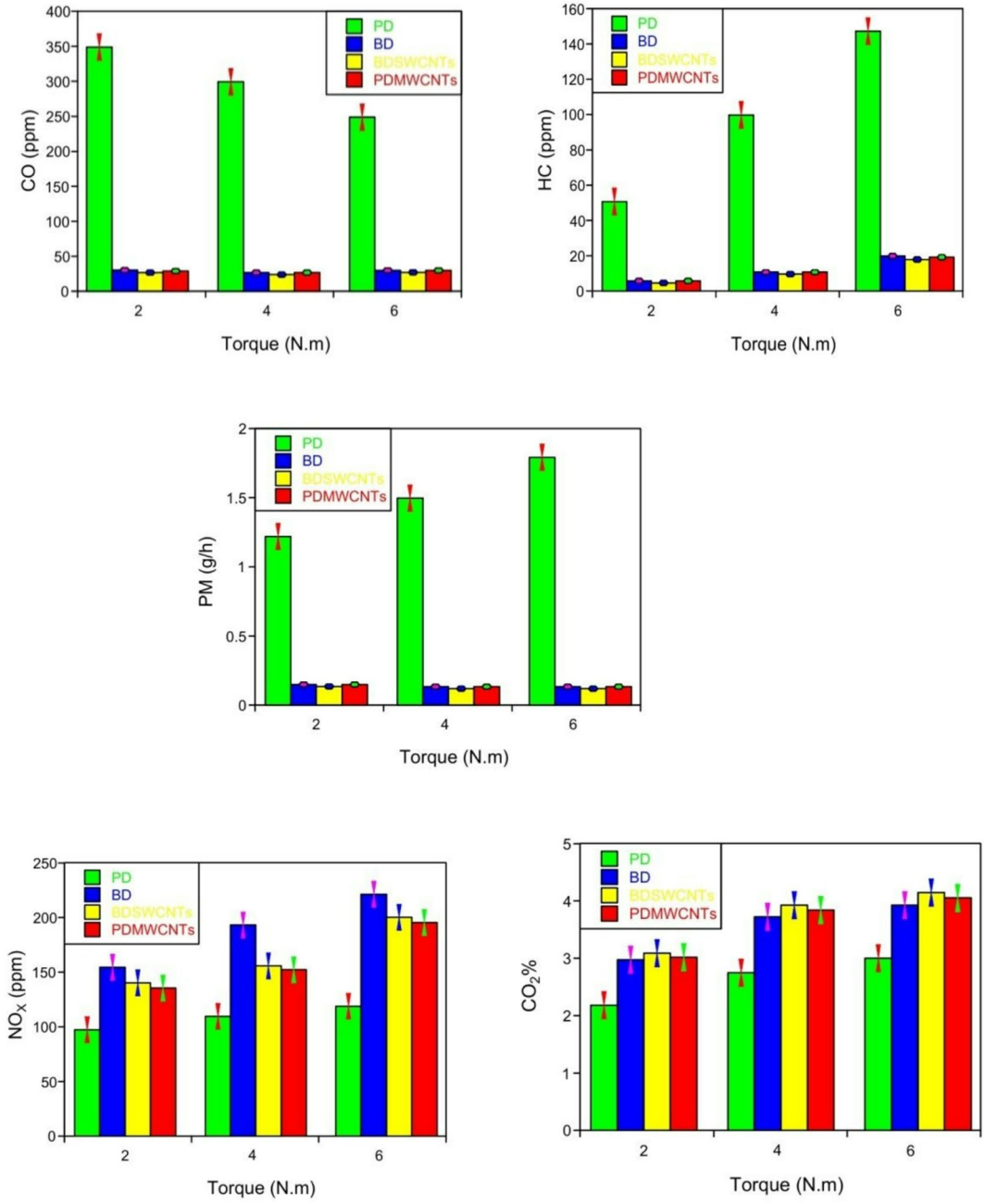

Fig. 8. Exhaust gas from engines running on different fuel types under different loads and maintaining a constant engine speed of 2000 rpm.

Sazhin et al.[48] attribute the release of hydrocarbons to the minimal participation of diesel in combustion and evaporation processes. The significant reduction in particulate matter emissions can likewise be attributed to the same rationale. The physicochemical features of fuel facilitate the emission of carbon monoxide during burning. In low-oxygen conditions, elevated partial combustion leads to increased carbon monoxide emissions. Consequently, biodiesel-derived fuels have an elevated oxygen content, resulting in reduced carbon monoxide emissions. The unique structure of multi-walled carbon nanotubes (MWCNTs) plays a key role in their thermal behavior. Their concentric layered design allows heat to dissipate radially, which helps moderate peak combustion temperatures[49]. This thermal regulation explains why MWCNT blends show 2–4% lower NOx emissions compared to single-walled nanotube formulations, as clearly shown in Fig. 9. Since NOx formation depends heavily on temperature, this thermal buffering effect proves particularly valuable.

Our surface area measurements tell an equally interesting story. BET analysis revealed SWCNTs have significantly more surface area (450 ± 20 m^2/g) compared to MWCNTs (220 ± 15 m^2/g). All that extra surface provides more active sites where oxidation reactions can occur. This helps explain why SWCNT blends performed

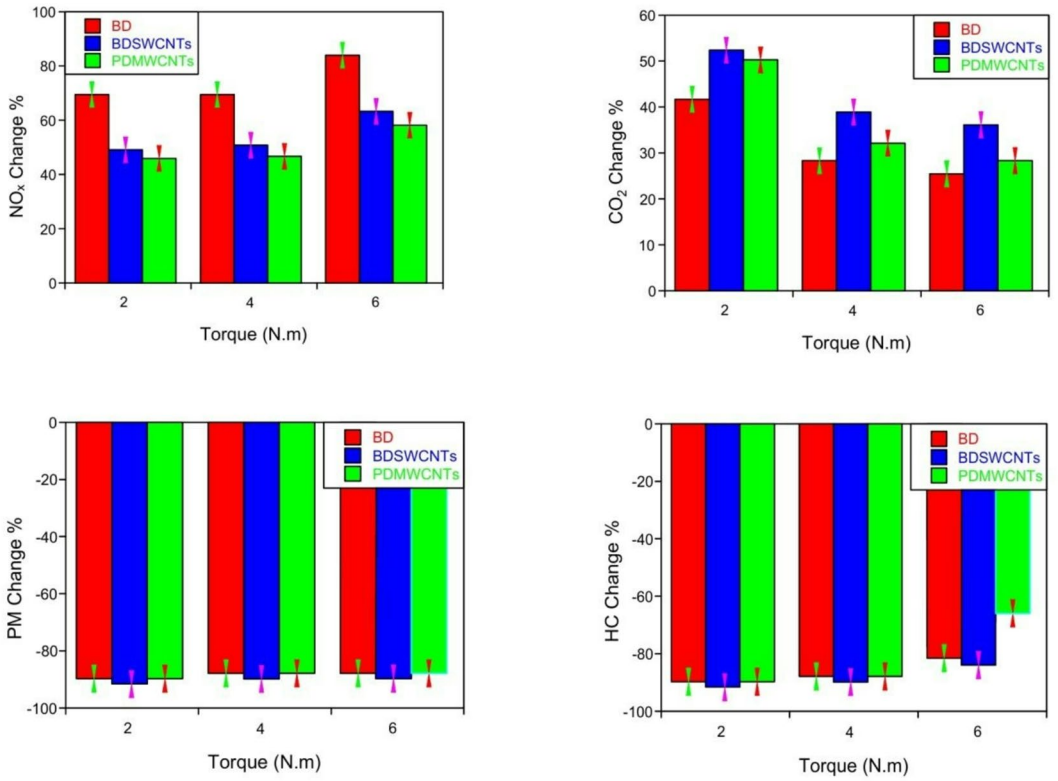

Fig. 9. shows how the percentage of released fumes changes when the engine is running at 2000 rpm and different loads are applied.

slightly better at reducing harmful emissions—they achieved 94% reduction in hydrocarbons versus MWCNTs' 92%, and 90.5% reduction in carbon monoxide compared to 89% for MWCNT formulations[50]

The observed reduction in HC, CO, and PM emissions, coupled with increased CO_2 production, indicates complete combustion when using BD and its nanoparticle blends (BD-SWCNT and BD-MWCNT) compared to PD. This enhanced combustion efficiency stems from the fuels' higher oxygen content, which promotes thorough oxidation of the fuel. While BD inherently leads to greater fuel consumption and CO_2 emissions than PD the incorporation of nanoparticles mitigates this effect by improving combustion efficiency, thereby limiting the increase in CO_2. The combined effects of elevated oxygen content, increased combustion temperatures, and higher engine torque collectively contribute to this optimized combustion behavior, where substantially reduced harmful emissions (HC, CO, PM) are achieved at the expense of a controlled rise in CO_2 output.

The increase in nitrogen oxide production indicates the impact of elevated combustion temperatures (Ozgen et al.[51]). Nitrogen oxides (NOx) are generated when atmospheric nitrogen dioxide interacts with oxygen derived from fuel, nanoparticles, or air. Increasing the combustion temperature and the concentration of accessible oxygen amplifies this process. To explain, at 2, 4, and 6 Nm, the NOx emissions of PD are 99.0, 108.4, and 116.7 ppm, respectively. The NOx emissions of BD are 159.0, 188, and 201 ppm, respectively. According to these data, using BD instead of PD increases NO emissions by around 75% at 2 and 4 Nm and by about 80% at 6 Nm. The incorporation of nanoparticles may reduce nitrogen oxide emissions. The disparity in NO emissions between MWCNT and SWCNT may be attributed to the decreased oxygen concentration in MWCNT. A detailed analysis reveals that at 2, 4, and 6 Nm, BDSWCNT produces 144.0, 169, and 196 ppm of NOx, respectively, while BDMWCNT emits 142.0, 160.0, and 190.0 ppm of NOx, as stated. The findings indicate that the percentages of NO emissions rose by 48.0%, 50.3%, and 62.5% with the application of BDSWCNT at 2, 4, and 6 Nm, respectively. The respective percentages of NO emissions with the usage of BDSWCNT were 48.3%, 45.6%, and 58.8%

Because SWCNT and MWCNT nanoparticles exhibit different physicochemical characteristics and catalytic behaviors when they are burned, it is possible to provide a mechanistic explanation for the changes in CO_2 and NOx emissions that are related to the use of these nanoparticles. It is well known that SWCNT when in its anatase form, has a considerable oxidizing capacity. This ability leads to increased combustion temperatures and improves fuel oxidation (Chen et al.[52]). Over the last several years, this characteristic has garnered considerable attention for SWCNTs. This increase in temperature facilitates the atmospheric reaction between nitrogen dioxide and oxygen, leading to a greater release of nitrogen oxides into the environment. However, the enhanced temperature conditions result in a larger production of NOx emissions. This is despite the increased oxygen content in SWCNT compared to MWCNT, which makes combustion more complete. MWCNT, in contrast to SWCNT, exhibits distinctive thermal properties and has a lower propensity to generate excessive heat. There is a reduction in peak temperatures as a result of the MWCNT's capacity to effectively dissipate heat from the exhaust after ignition, which in turn helps minimize the production of nitrogen oxides.

The Statistics above were applied to the data using analysis of variance (ANOVA) to determine the degree of dissimilarity between the means of more than two groups. This research was conducted to determine whether there was a discernible difference in the use of PD and BD derived from waste oils incorporating SWCNT and MWCNT nanoparticles. All *P* values are lower than 0.02, as shown by the results of the analysis of variance (ANOVA) presented in the Electronic Supplementary Materials (ESM) available online for this article. Because this demonstrates that all the observed changes contain significant improvements—and that these improvements are respectable—and are not merely random fluctuations, it provides strong support for the dependability of the observed data.

Several factors may influence the cost and scalability of biodiesel additives. Although the preceding research indicated that adding nanoparticles to BD increases its performance, there are several other aspects that could affect its affordability. The techniques for production, the availability of raw materials, and market demand are all constituents of this group of variables. Because both single-walled and multi-walled carbon nanotubes are easily accessible and can be manufactured through simple processes such as chemical precipitation and sol–gel techniques, it is not difficult to increase the production of these nanotubes for commercial use[53]. They are also widely available. It is necessary to compare these expenses to the benefits of increased fuel economy and reduced emissions in order to determine whether it is feasible from a financial standpoint to proceed with expanding this approach. The use of waste sunflower oil as a feedstock for biodiesel production encourages recycling and minimizes waste, which in turn reduces the negative environmental impact of waste sunflower oil. However, the addition of nanoparticles increases the cost of the fuel. A preliminary calculation suggests that the initial expense in nanoparticle manufacturing would be substantial; however, the advantages of reduced pollutants and improved fuel economy would more than offset this. The growing demand for cleaner fuels, in conjunction with the tightening of emission rules, provides further evidence that incorporating nanoparticles into biodiesel is a financially feasible choice.

When compared to traditional and alternative renewable liquid fuels, nanoparticle-enhanced biodiesel offers significant environmental advantages. Carbon nanotubes (SWCNT/MWCNT) may be used to reduce emissions more effectively in biodiesel. This is notably true for hazardous pollutants, including hydrocarbons (HC), carbon monoxide (CO), and particulate matter (PM), which can be reduced by up to 96%, 90.5%, and 96%, respectively, compared to petroleum diesel. Although the entire combustion process inevitably produces an increase in carbon dioxide emissions, this trade-off is environmentally justifiable due to the significant decrease in more detrimental emissions to the environment, such as pollutants and carbon monoxide. Biodiesel continues to pose a significant environmental hazard due to its oxygen-rich composition and high combustion temperatures, which lead to increased NOx emissions. These emissions are 45–80% higher than those from regular diesel. In contrast, other renewable energy sources, such as ethanol, often have lower NOx profiles and carbon footprints than the alternatives listed below. Nonetheless, the current study on nanoparticles shows that there is a possibility for reducing this issue. MWCNT blends have been demonstrated to reduce NOx levels by two to four percent more than unmodified biodiesel. When considering the whole lifetime, nanoparticle-enhanced biodiesel provides a compelling argument for long-term use. This is especially true when paired with innovative technologies for reducing NOx emissions, such as selective catalytic reduction or exhaust gas recirculation systems. As a result of the fuel's compatibility with the existing diesel infrastructure and its capacity to utilize a diverse range of feedstock sources, it enhances its position as a potential transitional fuel in the transition to carbon–neutral energy systems.

Conclusion

This experimental study demonstrates that waste cooking oil-derived biodiesel, when enhanced with carbon nanotube additives, presents a viable alternative fuel with significant environmental benefits. Our systematic investigation reveals three key findings:

The base biodiesel formulation achieved substantial emission reductions, decreasing hydrocarbon (HC) and carbon monoxide (CO) emissions by 89–95% compared to conventional diesel, while maintaining acceptable engine performance parameters. These improvements stem from the fuel's oxygenated molecular structure promoting more complete combustion.

The incorporation of carbon nanotubes (CNTs) effectively addressed several biodiesel limitations. Single-walled CNTs (SWCNTs) with their high surface area (450 ± 20 m^2/g) and tetragonal-anatase crystalline structure enhanced combustion efficiency by 3.7–6.4%. Multi-walled CNTs (MWCNTs) demonstrated superior heat transfer capabilities through their concentric layered structure, helping mitigate NOx emissions—a persistent challenge in biodiesel applications.

The study identified remaining technical challenges requiring further research, particularly the trade-off between reduced particulate emissions (95% decrease) and increased NOx levels (45–80% higher). The nanoparticle additives partially alleviated but did not eliminate this fundamental biodiesel characteristic.

These findings make significant contributions to sustainable fuel development by validating waste cooking oil as a practical and effective biodiesel feedstock, demonstrating its successful conversion into a viable fuel source while addressing waste management challenges. The study establishes optimal carbon nanotube (CNT) concentration ranges of 50–150 ppm that effectively enhance fuel performance, providing crucial guidance for future formulation development. Furthermore, the research generates valuable empirical data on nanoparticle-mediated combustion improvement, specifically quantifying how single-walled and multi-walled CNTs influence key parameters such as combustion efficiency (3.7–6.4% improvement), emission reduction (up to 95% decrease in particulate matter), and thermal management. These combined outcomes advance our understanding of nano-additive applications in alternative fuels and provide a scientific foun-

dation for developing more sustainable transportation energy solutions that balance environmental benefits with practical engine performance requirements.

Prospective research

In further research, the primary focus should be on identifying solutions to substantial empirical obstacles that arise during the development and implementation of nanoparticle-enhanced biodiesel. To begin, it is essential to conduct thorough lifecycle assessments to determine the overall environmental benefits, considering the rising levels of gaseous oxides and carbon dioxide emissions. It is vital to conduct a comprehensive evaluation under various storage conditions and for a short period to achieve the second objective, which is to establish the durability of nanoparticle dispersion in biodiesel over an extended period. Third, there is a need for a study to be conducted to evaluate the potential wear impact that nanoparticle residues in combustion chambers and fuel systems may have on engine durability. A comprehensive cost–benefit analysis is required to determine whether the manufacture of nanoparticles on a large scale and the modification of biodiesel are economically viable. In the fifth place, research needs to be conducted to determine the ideal quantities of nanoparticles that strike a balance between reducing pollution and improving engine performance under various operating conditions. Ultimately, research into the synergistic interactions between nanoparticles and NOx-reduction technology (such as EGR or SCR systems) may provide options to mitigate biodiesel's inherent environmental downsides while retaining its emission-reduction benefits for other pollutants. The advancement of these research areas is crucial for making the transition from laboratory accomplishments of nanoparticle-enhanced biodiesel to the development of engine solutions that are both functional and environmentally friendly.

Limitations

The study is limited by the short-term engine testing conditions, which may not reflect long-term operational effects.

Data availability

The datasets used and/or analysed during the current study available in the manuscript.

Received: 24 June 2025; Accepted: 5 September 2025
Published online: 08 October 2025

References

1. Çılğın, E. Synergistic effects of SWCNT and MgO nanoparticle additives on engine performance and emissions: A laboratory analysis approach. *Biofuels* **16**, 848 (2025).
2. Lopresto, C. G. Sustainable biodiesel production from waste cooking oils for energetically independent small communities: An overview. *Int. J. Environ. Sci. Technol.* **22**(3), 1953–1974 (2025).
3. Srinivasarao, M. et al. Combustion enhancement and emission reduction in an IC engine by adopting ZnO nanoparticles with calophyllum biodiesel/diesel/propanol blend: a case study of general regression neural network (GRNN) modelling. *Ind. Crops Products* **227**, 120812 (2025).
4. Sonachalam, M. et al. Experimental investigation of performance, emission, and combustion characteristics of a diesel engine using blends of waste cooking oil-ethanol biodiesel with MWCNT nanoparticles. *Case Stud. Therm. Eng.* **61**, 105094 (2024).
5. Tulashie, S. K. et al. A review on the production of biodiesel from waste cooking oil: A circular economy approach. *Biofuels* **16**(1), 99–119 (2025).
6. Lopresto, C. G., De Paola, M. G. & Calabrò, V. Importance of the properties, collection, and storage of waste cooking oils to produce high-quality biodiesel–An overview. *Biomass Bioenergy* **189**, 107363 (2024).
7. Bikkavolu, J. R., Vadapalli, S., Chebattina, K. R. R. & Pullagura, G. Investigation of the effect of adding carbon nanotubes, lower and higher level alcohol additives, in Yellow oleander methyl ester-diesel blend on diesel engine performance. *Energy Sources Part A: Recovery, Utilization, and Environmental Effects* **45**(4), 11619–11636 (2023).
8. Kumar, A., Pali, H. S. & Kumar, M. Evaluation of waste plastic and waste cooking oil as a potential alternative fuel in diesel engine. *Next Energy* **5**, 100181 (2024).
9. Kumbhar, V. S., Pandey, A., Varghese, A. & Patil, V. Comparative assessment of performance, combustion, and emission of compression ignition engine fuelled with different generations of biodiesel. *Int. J. Sustain. Eng.* **14**(6), 2082–2096 (2021).
10. Reşitoğlu, İA. & Keskin, A. The effect of biodiesel derived from waste oil on engine performance and emission characteristics. *J. Environ. Sci. Stud.* **1**(1), 55 (2018).
11. Kaisan, M. U. et al. Comparative analysis of experimental and simulated performance and emissions of compression ignition engine using biodiesel blends. In *Energy Recovery Processes from Wastes* 85–100 (Springer Singapore, Singapore, 2019).
12. Tesfa, B., Gu, F., Mishra, R. & Ball, A. Emission characteristics of a CI engine running with a range of biodiesel feedstocks. *Energies* **7**(1), 334–350 (2014).
13. Kannan, M., Sathish Babu, R. & Sathish, S. Experimental investigations on the performance and emission characteristics of CI engine fuelled with biodiesel from neem oil. *Int. J. Ambient Energy* **43**(1), 2351–2359 (2022).
14. Pullagura, G. et al. Performance, combustion and emission reduction characteristics of Metal-based silicon dioxide nanoparticle additives included in ternary fuel (diesel-SMME-iso butanol) on diesel engine. *Heliyon* **10**(4), e26519 (2024).
15. Devkota, L. K. & Adhikari, S. P. Experimental investigation on the performance of a CI engine fuelled with waste cooking oil biodiesel blends. *Himal. J. Appl. Sci. Eng.* **2**(1), 25–31 (2021).
16. Afzal, A. et al. Thermal performance of compression ignition engine using high content biodiesels: A comparative study with diesel fuel. *Sustainability* **13**(14), 7688 (2021).
17. Behera, B. N. & Hotta, T. K. Experimental studies on performance and emission measures of a 4-stroke compression ignition engine using palm bio-diesel blended with N-butanol. *J. Eng. Res.* **12**(4), 976–983 (2024).
18. Chuepeng, S., Komintarachat, C., Klinkaew, N., Maithomklang, S. & Sukjit, E. Utilization of waste-derived biodiesel in a compression ignition engine. *Energy Rep.* **8**, 64–72 (2022).
19. Krishania, N. et al. Investigations of spirulina, waste cooking and animal fats blended biodiesel fuel on auto-ignition diesel engine performance, emission characteristics. *Fuel* **276**, 118123 (2020).
20. Gautam, R. & Kumar, S. Performance and combustion analysis of diesel and tallow biodiesel in CI engine. *Energy Rep.* **6**, 2785–2793 (2020).

21. Arunprasad, S. & Balusamy, T. Experimental investigation on the performance and emission characteristics of a diesel engine by varying the injection pressure and injection timing using mixed biodiesel. *Int. J. Green Energy* **15**(6), 376–384 (2018).
22. Bikkavolu, J. R., Vadapalli, S., Chebattina, K. R. R. & Pullagura, G. Effects of stably dispersed carbon nanotube additives in yellow oleander methyl ester-diesel blend on the performance, combustion, and emission characteristics of a CI engine. *Biofuels* **15**(1), 67–80 (2024).
23. Pullagura, G., Bikkavolu, J. R., Prasad, V. V. S., Prathipati, R. & Seepana, P. Energy, exergy, and sustainability assessments of a compression ignition diesel engine fueled with Pongamia pinnata oil–diesel blends and nanoparticles. *Emergent Mater.* **8**(1), 199–215 (2025).
24. Jannatkhah, J., Najafi, B. & Ghaebi, H. Energy-exergy analysis of compression ignition engine running with biodiesel fuel extracted from four different oil-basis materials. *Int. J. Green Energy* **16**(10), 749–762 (2019).
25. Rajpoot, A. S., Saini, G., Chelladurai, H. M., Shukla, A. K. & Choudhary, T. Comparative combustion, emission, and performance analysis of a diesel engine using carbon nanotube (CNT) blended with three different generations of biodiesel. *Environ. Sci. Pollut. Res.* **30**(60), 125328–125346 (2023).
26. Gad, M. S., Aziz, M. M. A. & Kayed, H. Performance, emissions and exergy analyses of adding CNTs to various biodiesel feedstocks. *Propuls. Power Res.* **11**(4), 511–526 (2022).
27. Vellaiyan, S. et al. Characterization and optimization of waste-derived biodiesel utilizing CNT/MgO nanocomposite and water emulsion for enhanced performance and emission metrics. *Case Stud. Therm. Eng.* **55**, 104173 (2024).
28. Hoekman, S. K. & Robbins, C. Review of the effects of biodiesel on NOx emissions. *Fuel Process. Technol.* **96**, 237–249 (2012).
29. Hosseini, S. H., Taghizadeh-Alisaraei, A., Ghobadian, B. & Abbaszadeh-Mayvan, A. Performance and emission characteristics of a CI engine fuelled with carbon nanotubes and diesel-biodiesel blends. *Renew. Energy* **111**, 201–213 (2017).
30. El-Seesy, A. I., Abdel-Rahman, A. K., Bady, M. & Ookawara, S. J. E. C. Performance, combustion, and emission characteristics of a diesel engine fueled by biodiesel-diesel mixtures with multi-walled carbon nanotubes additives. *Energy Convers. Manage.* **135**, 373–393 (2017).
31. Soudagar, M. E. M. et al. The effect of nano-additives in diesel-biodiesel fuel blends: A comprehensive review on stability, engine performance and emission characteristics. *Energy Convers. Manage.* **178**, 146–177 (2018).
32. Ghafoori, M. et al. Effect of nano-particles on the performance and emission of a diesel engine using biodiesel-diesel blend. *Int. J. Autom. Mech. Eng.* **12**, 3097 (2015).
33. Khan, N. R. & Rashid, A. B. Carbon-based nanomaterials: a paradigm shift in biofuel synthesis and processing for a sustainable energy future. *Energy Convers. Manag.: X* **22**, 100590 (2024).
34. Wu, Y. et al. A review on current scenario of Nanocatalysts in biofuel production and potential of organic and inorganic nanoparticles in biohydrogen production. *Fuel* **338**, 127216 (2023).
35. Sulakhi, K. et al. Effects of metal-oxide nanoparticles and biodiesel mixtures on combustion, performance, emissions, vibration, and noise parameters in a variable compression ratio (VCR) diesel engine. *Case Stud. Therm. Eng.* **73**, 106692 (2025).
36. Azam, M. A. & Seman, R. N. A. R. Analysis and characterization of carbon nanotube. In *Graphene, Nanotubes and Quantum Dots-Based Nanotechnology* 333–355 (Woodhead Publishing, 2022).
37. Banerjee, S. & Kar, K. K. Characteristics of carbon nanotubes. In *Handbook of Nanocomposite Supercapacitor Materials I: Characteristics* 179–214 (Springer International Publishing, Cham, 2020).
38. Sarıdemir, S., Polat, F. & Ağbulut, Ü. Improvement of worsened diesel and waste biodiesel fuelled-engine characteristics with hydrogen enrichment: A deep discussion on combustion, performance, and emission analyses. *Process Saf. Environ. Prot.* **184**, 637–649 (2024).
39. Alçelik, N., Sarıdemir, S., Polat, F. & Ağbulut, Ü. Role of hydrogen-enrichment for in-direct diesel engine behaviours fuelled with the diesel-waste biodiesel blends. *Energy* **302**, 131680 (2024).
40. Islam, M. A. et al. Advances and significances of carbon nanotube applications: A comprehensive review. *Eur. Polym. J.* **220**, 113443 (2024).
41. Elkelawy, M., Draz, A. M., Seleem, H. E. & Hamouda, M. A. Performance characteristics of diesel engine power plants: efficiency, emissions, and operational flexibility. *Pharos Eng. Sci. J.* **2**(1), 1–11 (2025).
42. Wasiu, S., Aziz, R. A. & Megat, P. Brake specific energy consumption (BSEC) and emission characteristics of the direct injection spark ignition engine fuelled by hydrogen enriched compressed natural gas at various air-fuel ratios. *Int. J. Appl. Eng. Res.* **13**(1), 677–683 (2018).
43. Zheng, F. & Cho, H. M. The comprehensive effects of nano additives on biodiesel engines—A review. *Energies* **17**(16), 4126 (2024).
44. Wang, X., Aloufi, A. S., Gavurová, B., Le, Q. H. & Brindhadevi, K. Assessment of noise and vibration characteristics of Botryococcus braunii microalgae and hydrogen blends in internal combustion engines for highway vehicles. *Fuel* **355**, 129502 (2024).
45. Truong, T. T. et al. Effect of alcohol additives on diesel engine performance: A review. *Energy Sour. Part A: Recov. Util. Environ. Effects* **47**(2), 2011490 (2025).
46. Li, R. et al. Effects of cetane number improvers on the performance of diesel engine fuelled with methanol/biodiesel blend. *Fuel* **128**, 180–187 (2014).
47. Bikkavolu, J. R., Pullagura, G., Vadapalli, S., Chebattina, K. R. & Pathem, U. C. Influence of nano additives on performance, combustion, and emission characteristics of diesel engine using tamarind oil methyl ester-diesel fuel blends/Bikkavolu Joga Rao… [et al.]. *J. Mech. Eng. (JMechE)* **20**(3), 313–333 (2023).
48. Al Qubeissi, M. et al. Heating and evaporation of droplets of multicomponent and blended fuels: A review of recent modeling approaches. *Energy Fuels* **35**(22), 18220–18256 (2021).
49. Rao, B. J., Srinivas, V., Rao, C. K. R. & Gandhi, P. Thermogravimetric analysis and injection pressure strategies on a CI engine using yellow oleander methyl ester-diesel blends with nano additions. *Emergent Mater.* **7**(3), 847–866 (2024).
50. Rao, B. J., Pullagura, G., Vadapalli, S., & Chebattina, K. R. R. (2023, December). The effect of CNTs on physicochemical properties of yellow oleander biodiesel-diesel fuel blends. In *AIP Conference Proceedings* (Vol. 2943, No. 1, p. 020017). AIP Publishing LLC.
51. Ozgen, S., Cernuschi, S. & Caserini, S. An overview of nitrogen oxides emissions from biomass combustion for domestic heat production. *Renew. Sustain. Energy Rev.* **135**, 110113 (2021).
52. Chen, A. F. et al. Combustion characteristics, engine performances and emissions of a diesel engine using nanoparticle-diesel fuel blends with aluminium oxide, carbon nanotubes and silicon oxide. *Energy Convers. Manage.* **171**, 461–477 (2018).
53. Zhang, Q., Huang, J. Q., Qian, W. Z., Zhang, Y. Y. & Wei, F. The road for nanomaterials industry: A review of carbon nanotube production, post-treatment, and bulk applications for composites and energy storage. *Small* **9**(8), 1237–1265 (2013).

Author contributions

Mohammed Azarudeen J: Conceptualization and methodology.Anish M: Data curation and formal analysis.L. Ganesh Babu: Supervision and validation.A. R. Sivaram: Software.N. Punitha: Resources and data collection. Karthick Muniyappan: Writing – original draft preparation.Jayant Giri: Visualization and review.Mohammad Kanan: Writing – review and editing.Jayaprabakar Jayaraman: Project administration and funding acquisition.S. Baskar: Investigation.

Funding
This research work is not funded by any one.

Declarations

Competing interests
The authors declare no competing interests.

Additional information
Correspondence and requests for materials should be addressed to M.A. or M.K.

Reprints and permissions information is available at www.nature.com/reprints.

Publisher's note Springer Nature remains neutral with regard to jurisdictional claims in published maps and institutional affiliations.